

# Petrographic Characteristics and Fluid Inclusion Study of Carbonate Cements in Permian-Triassic Rock Sequence of Southern Iran: an Implication of Rock-fluid Interactions in Carbonate Reservoir Rocks

Pouran Nazarian Samani\*, Maryam Mirshahani, and Navab Khodaei

Petroleum Geology Division, Research Institute of Petroleum Industry, Tehran, Iran

## ABSTRACT

The study of the carbonate cements in the Permian-Triassic Dalan-Kangan formations resulted in the identification of five stages of calcite and dolomite cementation, which completely or partially occluded pores. Cement types appear to be early isopachous calcite (i; C1-non-luminescence), equant (ii; C2-dull CL), fairly coarse secondary dolomite rhombs (iii; C3-zoning red CL), coarse sparry calcite (iv; C4-dull CL), and meteoric equant calcite (v; C5-bright orange CL & vi; C6-bright yellow CL). Fluid inclusion analyses invoked three distinct groups of fluids. Group 1 is reflected by fluids with equant calcite (C2) composition, characterized by Th values (126 °C) and salinity of 16 wt.% (NaCl equivalent), and they are interpreted as burial pore-waters. Group 2, which is represented by fluids associated to shallow burial dolomite cementation (C3), has Th values about (127 °C) and salinity of 17 wt.% (NaCl equivalent). The last group, i.e. coarse sparry calcite (C4), is occurred along fractures and vugs and characterized by high Th values (169 °C) and salinity of 17.5 wt.% (NaCl equivalent) which shows that fluids with a higher temperature migrated from deeper parts during deep burial. The hydrocarbon inclusions with yellow fluorescence can be observed in coarse calcite filling fractures in Dalan formation which shows that they are secondary, and hydrocarbon migration predates the precipitation of fracture filling cements.

**Key words:** Diagenesis, Fluid Inclusion, Kangan, Dalan.

## INTRODUCTION

The hydrocarbon reservoirs of the upper Dalan and Kangan (“Khuff equivalent”) formations hold some of the most important gas reservoirs in the world [1]. This is demonstrated by the South Pars in Iran and North Dome Gas field in Qatar, which is the largest offshore gas field in the world and is estimated to have over 1100 trillion cubic feet

of gas initially-in-place (TCF GIIP) [2]. In particular, the upper Dalan-Kangan reservoirs of onshore and offshore Iran contain some of the largest gas fields in the Middle East region [3]. Recently, these rock sequences, in both outcrop and subsurface, have been more or less well-documented in Iran [4-5] and like their equivalents in Abu Dhabi and Saudi Arabia [6-7].

### \*Corresponding author

Pouran Nazarian Samani  
Email: samanip@ripi.ir  
Tel: +98 21 4825 2447  
Fax :+98 21 4473 9723

### Article history

Received: November 07, 2015  
Received in revised form: March 12, 2016  
Accepted: May 25, 2016  
Available online: July 22, 2017

The studied area is one of the gas fields in the Persian Gulf (Figure 1). More than 60% of the reservoir rock at this field is dolomitized, and anhydritization occurs in close association with the dolomites, reflecting the influence of hypersaline depositional conditions on both calcium sulfate precipitation and dolomitization [8]. This study is conducted to recognize different carbonate cements (calcite and dolomite) occluding the pore spaces, and to document the fluid flow and diagenetic evolution in the Permian-Triassic Dalan-Kangan carbonate reservoirs in the southern Iran. Calcite and dolomite cements formed during burial are found in many carbonate reservoirs [9], associated with chemical compaction commonly occluded porosity to varying degrees in the investigated rock successions. On the contrary, early diagenetic processes such as aragonite dissolution and host rock dolomitization in addition to depositional facies are believed to have played a prominent role in fortifying the porosity and permeability of Dalan-Kangan carbonates reservoir [5, 7, 8, 10, 11, 12, 13, 14, 15]. In this paper, the entire Permian-Triassic reservoir succession is studied in point of petrographic, cathodoluminescence (CL), and fluid inclusion micro-thermometry to reveal: 1) the origin and geochemical evolution of fluids; and 2) the timing of the formation of different cements and their circulation within the studied succession.

## EXPERINTAL PROCEDURES

### Geological Setting

During the Permian, a shallow restricted evaporite-carbonate platform covered most of the Persian Gulf region [1]. Short-term sea level fluctuations caused recurrent shoaling pulses which culminated in the creation of evaporite sabkha and salinas particularly over highs. The carbonates indicate a shallow-shelf to a coastal-plain depositional environment. In general, a prograding terrigenous to shallow-marine clastic shoreline existed. The sediments of the late Early

Permian on the Arabian plate are characterized by regressive sediments such as the Unayzah (A and B) formation. Dolostones appear to constitute most of the Permian rock sequence in the Persian Gulf region. At the end of the Early Permian time, a major marine transgression resulted in the establishment of carbonate platform over much of the region. Following the widespread carbonate deposition during Late Permian [2], arid and semi-arid climate conditions are characterized by the Triassic succession (Figure 2). There was an increase in periodic shallow water carbonate deposition commonly interbedded with anhydrite. After uplift and rifting, shallow-marine conditions became dominant during the Late Triassic time [2].

Sedimentation continued without interruption or facies changes throughout the Permian-Triassic boundary in the Persian Gulf region particularly in the northern regions [16]. The Upper Permian-Triassic carbonate and evaporites of the Persian Gulf basin accumulated on an epeiric shelf.

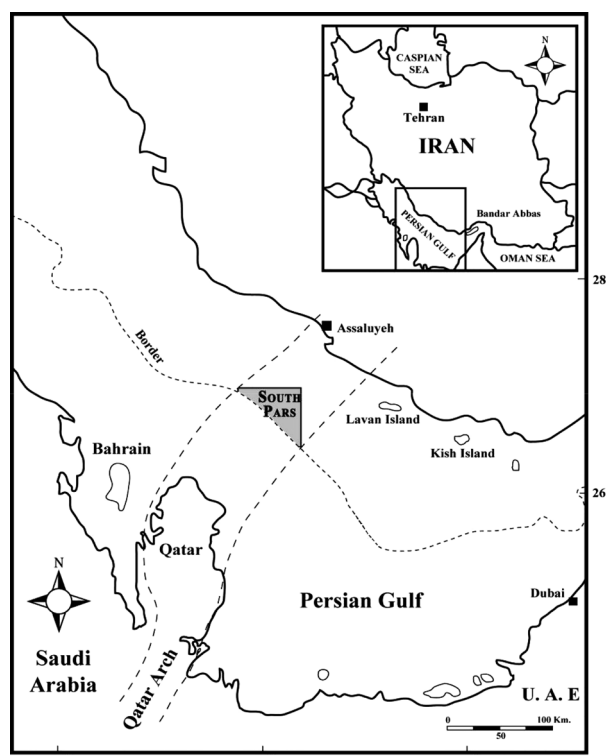


Figure 1: The location of the studied gas field in the Iranian portion of the Persian Gulf is marked by a grey triangle.

interrupted periodically by a series of transgressive and regressive events. In the Zagros basin to the southeast and across the Persian Gulf to northern Oman, thick Permian carbonates pass upward into Triassic carbonates (Figure 2). Hence, the continuous Upper Permian-Lower Triassic carbonates may act as a single reservoir, especially where overlying Triassic Dashtak evaporites served as a caprock [3, 5, 17].

Dalan formation has a total thickness of 600 meters consisting of medium to thick-bedded oolitic to micritic shallow-marine carbonates, locally reefal, with intercalations of evaporites. It extends up into the Lower Triassic Kangan formation in the southern Iran. Moreover, Dalan formation is subdivided into four reservoir units, including K5 (lower Dalan), Nar member, K4, and K3 (upper Dalan), which overlies the Faraghun formation (Figure 2). The transgressive lower Dalan formation was deposited in a more open marine environment as indicated by the presence of the open marine fossils. However, with depositional progradation and less subsidence, the depositional environment became progressively restricted. This eventually led to the deposition of evaporites in the Permian Sea. The main parts of the Dalan carbonates were deposited as a restricted evaporitic, carbonate shelf facies and include subtidal carbonate sand shoals, lagoons, and bars that spread out as sheets across long distances, along with intertidal and supratidal sabkha facies.

Kangan formation represents the first transgression of the Triassic Sea in the Zagros and the northern Persian Gulf region. Subdivided into two reservoir units (K2 and K1), Kangan formation overlays uncomfortably on Dalan formation (Figure 2), and passes upward into the Aghar shale member of Dashtak formation. A more or less fossil-barren zone is visible at the base of Kangan, which is followed by microbial mats and thrombotic beds across the Zagros basin and Arabian Peninsula

[1]. This marker bed specifies the Lower Kangan formation. Kangan formation correlates with Khuff-A member and the lower part of Khuff-B in the southern Persian Gulf [18]. The carbonate sequences and the evaporite facies were deposited in an arid homoclinal ramp platform, with the environmental conditions changing from sabkha to open marine settings.

## Methodology

About 900 thin-sections were prepared from the core samples of the upper Dalan and Kangan formations and were used to describe petrographically. The thin-sections were treated with Alizarin-red-s following Dickson [19] methodology. Standard petrographic analyses on the stained thin sections were carried out to aid the recognition of calcite and dolomite cementing phases. Cathodoluminescence was applied to determine different generations of cements using a Cold System CL Microscope (model 8200 MK4). For this study, 30 samples were selected to prepare the polished thin section. The study was conducted by means of CL apparatus in the RIPI laboratory in 15 kv and 400  $\mu$ A conditions.

Fluid inclusions were analyzed petrographically using the methods of Burruss [20]. Micro thermometric data were collected by standard techniques [21, 22], and the equation of Bodnar [23] was used to convert final ice melting temperatures ( $T_m$ ) to salinity. For this study, 30 samples were selected for preparing the doubly-polished thick sections, and micro thermometry was carried out on 11 samples using a Linkam THM600 heating-cooling stage and the controller attached to an Olympus petrographic microscope in the RIPI laboratory; the precision was 0.05 °C. The phase transition temperatures measured are calibrated using synthetic inclusions and pure chemicals obtained commercially which are accurate to better than 1.2 °C between 0 °C and 300 °C, and better than 0.3

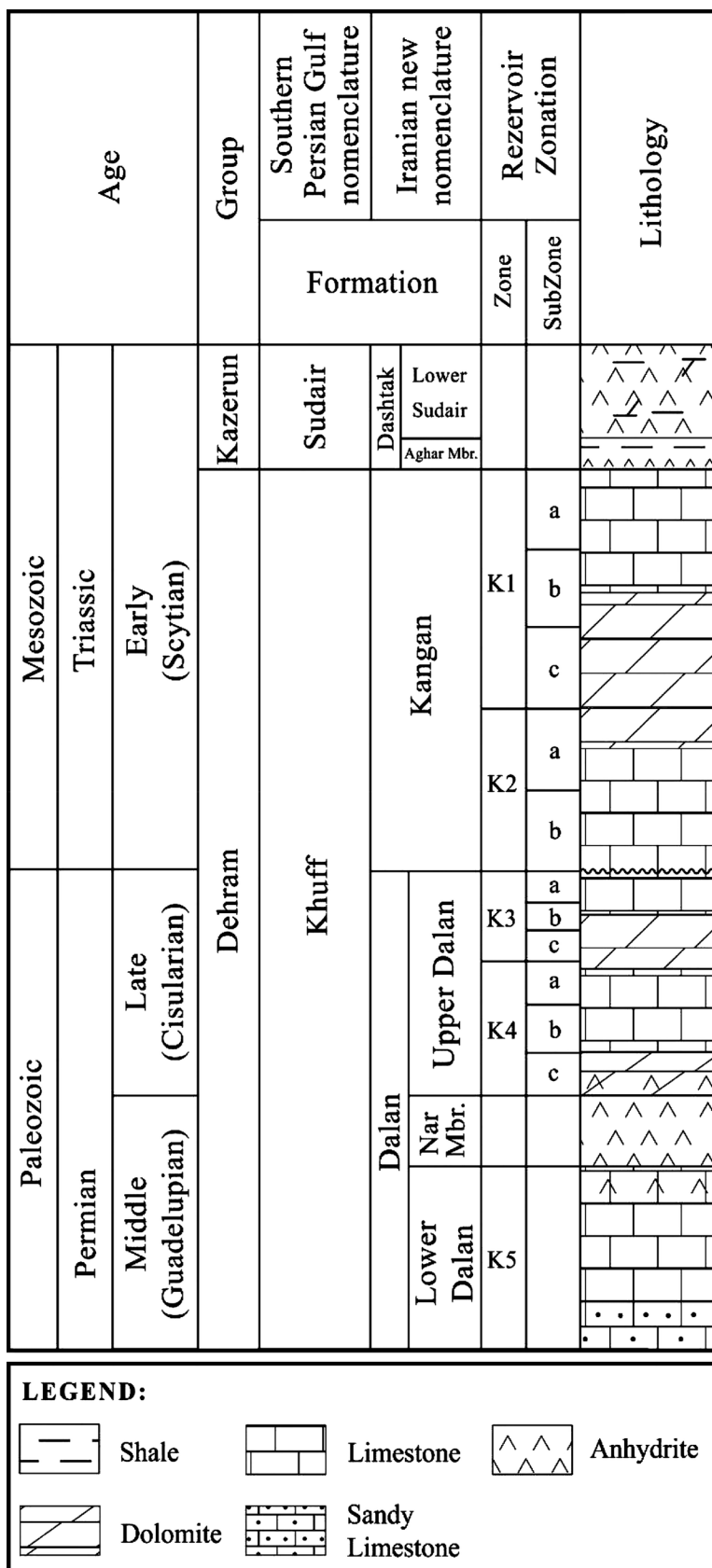


Figure 2: Stratigraphic nomenclature for Permian-Triassic (and underlying) rocks in Iran (modified after [5]).

°C between -150 °C and 0 °C. To measure these temperatures, small inclusion-bearing portions were cut from the wafers and, for each piece, homogenization temperatures were measured in an increasing order before any freezing runs. This minimizes the risk of stretching or bursting the inclusions before the data have been obtained. Petroleum and aqueous inclusions were identified under a combination of incident UV and transmitted plane polarized light on a standard petrographic microscope. API gravities of fluorescent petroleum inclusions were estimated from a correlation of their visible range spectra with spectra from a calibration set of 67 reservoir oil and condensates, spanning the API range of 10-60°. The spectra were obtained using an Olympus UMSP50 spectrometer with a barrier filter at 395 nm, scanning a diffraction grating at 4 nm intervals. Variable sized aperture masks allow spectra to be obtained from individual inclusions.

## RESULTS AND DISCUSSION

### Petrography and Cathodoluminescence

Kangan and Dalan carbonates are extremely susceptible to mineralogical and textural change, cementation, and dissolution. These alterations can occur at any time from initial deposition to deep burial [24-25]. Moreover, the diagenesis of carbonates can take place in many settings: the marine environment during deposition of the sediment, near the sediment surface where fresh waters penetrate the sediments, or in deeper subsurface. In addition, diagenetic changes may affect porosity, so they must be considered for better exploration in carbonates. Cementation is a major diagenetic process affecting carbonate sediments and rocks in Kangan and Dalan formations in a studied well. Cementation comprises processes leading to the precipitation of minerals in primary or secondary pores and requires the super

saturation of pore fluids with respect to the minerals [26]. Cementation is the main result of the chemical precipitation of a binding agent or the chemical welding of adjacent detritus grains. In this case, a chemical precipitate, usually calcium carbonate, fills the pores [27]. Sometimes dolomite precipitates between pore spaces as an initial mineral and acts as a binding agent between the grains. The bulk and mineral compositions change slowly during diagenesis in response to changes in pore water chemistry; thus, they can provide perception in the rock-fluid interaction evolution. Subsequently, various types of cements at different times can be distinguished in the Dalan and Kangan formations. These cements include calcite, anhydrite, and dolomite cements which partially or completely have filled pore spaces. The common type of carbonate cements which has affected the pores are isopachous, granular equant, and coarse blocky dolomite cement.

### Isopachous Cement

Isopachous rim cement (C1) forms as a relatively thin film around skeletal grains. This type is not mostly disseminated and appear in many cases leached, indicating a primary metastable mineralogy [28-29]. The nature of this calcite phase indicates precipitation in the marine-phreatic environment, where all pore spaces are filled with marine water [30]. It mostly appears on the outer and inner surfaces of micritized bioclasts, forming an isopachous coating of a variable size (Figures 3A, 3C, and 3H). Under CL, the isopachous cement is non-luminescent.

### Granular Calcite

The granular equant calcite cement occurred as pore filling material occluding different types of pore spaces, including fractures (Figure 3E), interparticle pore spaces (Figure 4F), and intraparticle pore spaces

(Figure 3C). Under a cross-polarized light, clear calcite crystals show a straight extinction. Most aragonitic ooids, foraminiferas, and molluscs are represented by molds occupied with granular calcite. The precipitation of this cement type occurred after a period of dissolution, where gastropods, some aragonitic ooids, and foraminiferas have been dissolved. Cement crystals in pores generally increase in size from pore boundary toward pore center (Figure 3G). Granular calcite cements overlay the cloudy isopachous calcite cements (Figure 3H). The granular equant calcite cement have variable luminescence patterns, from dull red, C2, (Figures 4C and 4G), to bright orange, C5, (Figures 4A and 4C), and to brightly yellow, C6, (Figure 4E) luminescent zones, indicating that it was formed under different fluid compositions. By an optical conventional microscope view, equant calcite cements (types C5 and C6), the bright light orange, and yellow luminescent appear to have been formed after the precipitation of dolomite (C3) cements (Figures 3D and 3G and Figure 4C). They appear to be the last cement generations and have petrographic characteristics [31-32] and cathodoluminescent characteristics similar to those of meteoric-phreatic origin.

### Coarse Blocky

Coarse blocky cement (C4) occurs as a pore filling material occluding all types of pore spaces including fractures, interparticle pore spaces, and vuggy porosities (Figures 3F and 3H, Figures 4E and 4F). Late stage, deep burial cement crystals are commonly large crystals filling more than one interparticle pore space, fracture, and molds. They have dull luminescent (Figure 4E).

### Dolomite Cement

By secondary dolomitization, dolomite cement occurred in some molds and vugs (Figures 3B, 3D, 3F, and 3G) in Kangan and Dalan formations, which reveals red zoning luminescent pattern (Figure 3G

and Figure 4C). According to the witness coming through microscopic analyses, dolomite crystals postdate the equant C2 and predate coarse blocky calcite C4 (Figure 3F) and equants C5, C6 (Figures 3G and 4C).

### Fluid Inclusion Study

Calcite cements, including types C2 and C4 with dolomite cement C3 from the investigated Kangan and Dalan rocks were selected for fluid inclusion analyses. Fluid inclusion assemblages (FIAs) were taken in defining and representing the groups of fluid inclusions that presumably trapped at about the same time [21-22]. The second step involves verifying the fluid inclusions composition (aqueous or hydrocarbon inclusion). Table 1 provides a listing of the analyzed samples within the studied formations. Under UV, most hydrocarbon filled inclusions fluoresce, revealing a particular color depending on the maturity of the hydrocarbon. Aqueous inclusions do not fluoresce [20-32].

Petrographic observation showed that all of fluid inclusions within calcite cements (pore-filling and fracture-filling) were two-phase aqueous inclusions, while in dolomite cements, two types of inclusions were identified: two-phase aqueous inclusions and hydrocarbon inclusions. The homogenization temperature ( $T_h$ ) and final ice-melting temperature ( $T_{m_{ice}}$ ) of aqueous inclusions were measured on the some cement samples. The micro thermometric measurements of fluid inclusions for some of these samples were impossible because of their size. Based on petrographic and fluid inclusion analyses, fluids responsible for these cement precipitations in Kangan and Dalan formations can be subdivided into three groups. Group 1 is the fluid responsible for the precipitation of equant II calcite ( $T_h$  values: 107.2 °C-136.8 °C, mean=126 °C; mean salinity= 16 wt.% (NaCl equivalent)). Group 2 represents a dolomitizing

fluid that has a Th value in the range of 107.2°C to 139.3 °C (with a mean at 127 °C) and mean salinity of 17 wt.% (NaCl equivalent). The last fluid inclusion analysis occurring along fractures is characterized by

high Th values (155.4°C-181.2°C, mean=169 °C) and mean salinity of 17.5 wt.% (NaCl equivalent). These identified groups are characterized by their specific Th and salinity values of primary inclusions (Figure 5).

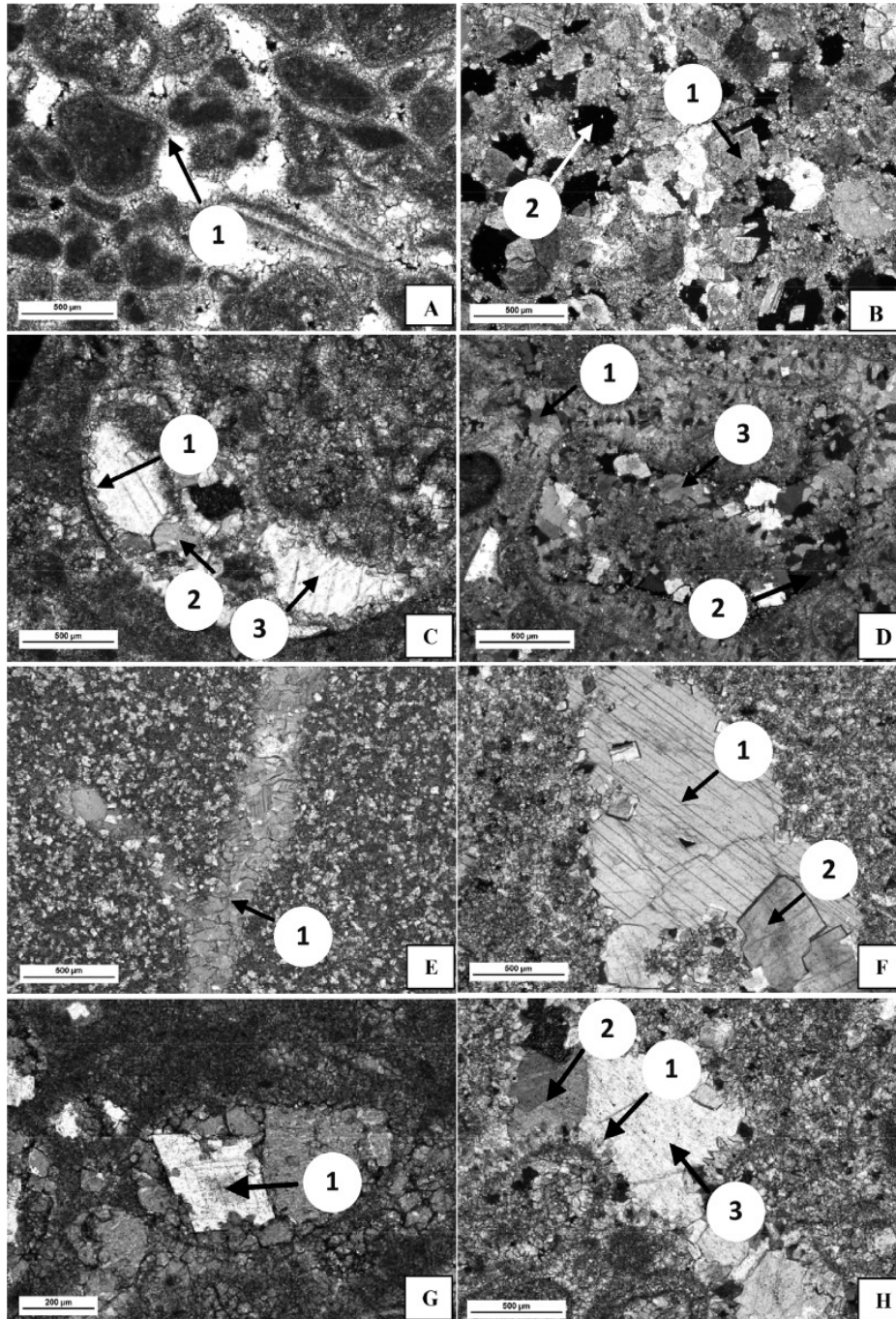


Figure 3: A- Early isopachous rime calcite cement (arrow no. 1), PPL. B-Coarse dolomite cement (arrow no. 1), moldic porosity resulting of dissolution (arrow no. 2) XPL. C-Isopachous rim (arrow no. 1), equant (arrow no. 2), coarse burial (arrow no. 3) cements, XPL. D-equant (arrow no. 1), coarse calcite (arrow no. 2), coarse dolomite cement (arrow no. 3), XPL. E- equant filling fracture (arrow no. 1), PPL. F-coarse burial calcite (arrow no. 1), coarse dolomite (arrow no. 2), XPL. G-granular calcite cement increased in size toward the center, coarse zoned dolomite cement (arrow no. 1) was predated and affected by equant calcite, PPL. H-Isopachous filling (arrow no. 1), equant (arrow no. 2) and coarse burial cement (arrow no. 3), XPL.

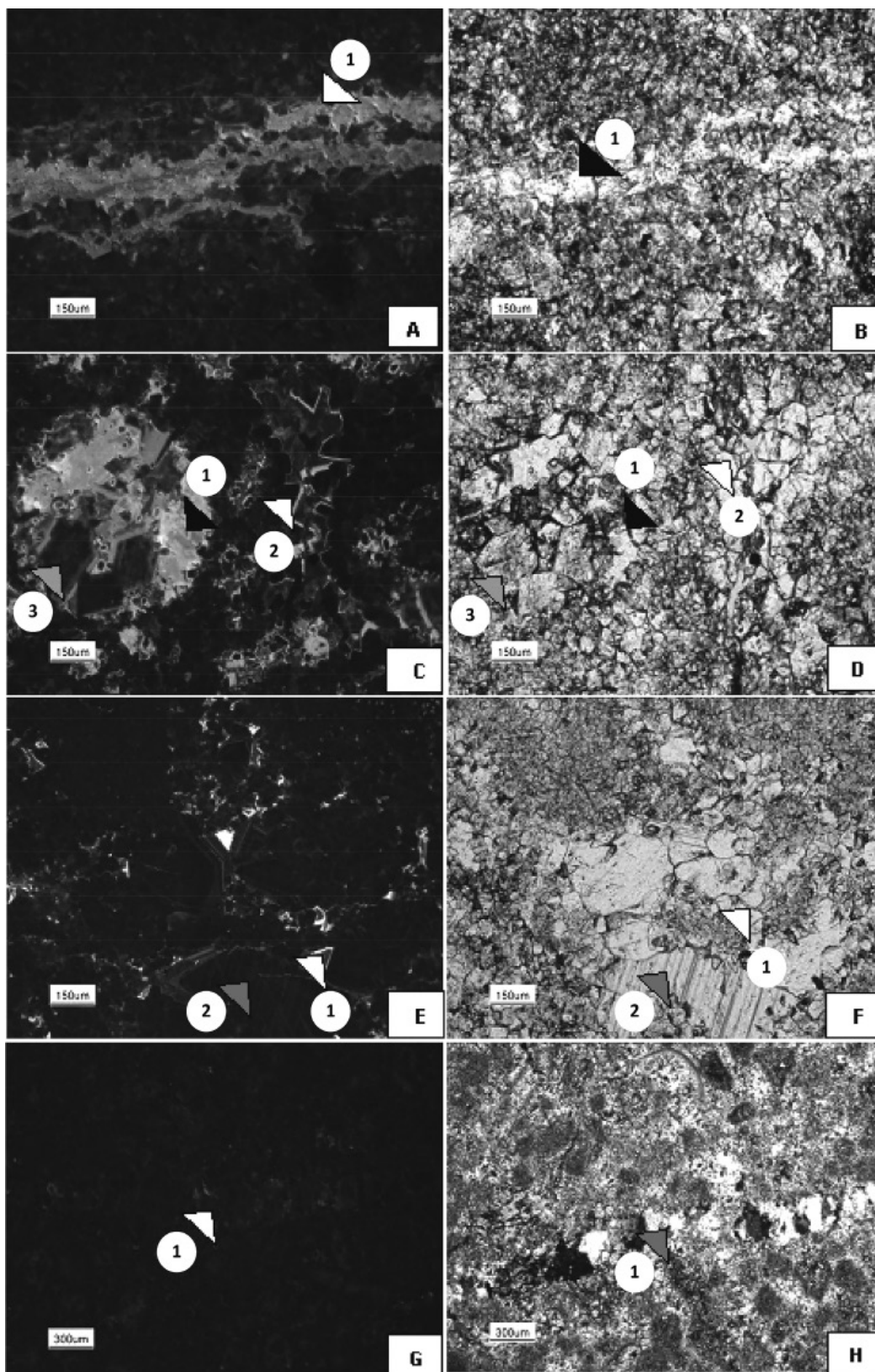
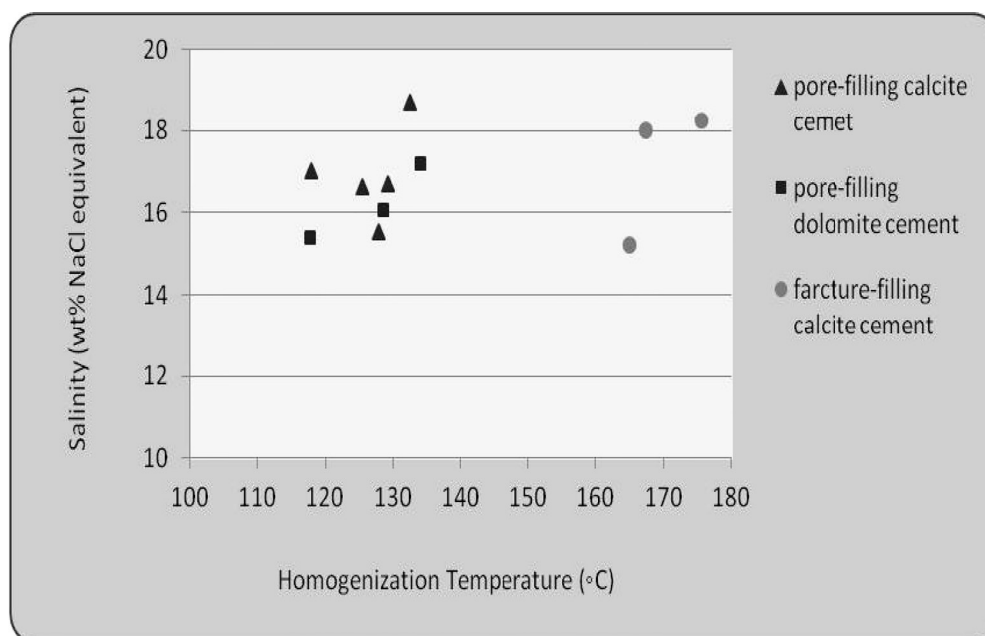


Figure 4: A and B- Granular equant II calcite filling fracture, bright orange CL (arrows no. 1) PPL and. C and D- equant II (arrow no. 1), equant (arrow no. 2) dull red, coarse dolomite (arrow no. 3) red luminescence, corroded dolomite crystals by equant calcite II and III, XPL. E and F- equant III (arrow no. 1) yellow luminescence, coarse burial calcite (arrow no. 2) dull CL, PPL. G and H- fracture filling equant I (arrow no. 1) dull red luminescence and red arrow in XPL view.

In conformity with salinity and temperature results, Fontana has reported similar data from dolomite and coarse sparry calcite cements in the Upper Permian-Lower Triassic Khuff formation [7]. Hydrocarbon

inclusions were observed in three samples. All of these samples belong to Dalan formation, and they show yellow fluorescence. Some of photomicrographs of aqueous and hydrocarbon inclusions are shown in Figure 6.



**Figure 5:** A cross plot of homogenization temperature (Th) and salinity values (wt.% NaCl equivalent) of fluid inclusions measured from coarse-crystalline calcite and dolomite cements from Kangan and Dalan Formations. Each point shows a fluid inclusion assemblages (FIAs), representing of the groups of fluid inclusions that presumably trapped at about the same time.

### Impacts on Reservoir Characteristics

Previous studies have investigated the impact of diagenesis on porosity evolution in the Permian-Triassic carbonates of the Arabian Plate (see for example references [34-35]), and this has been well-documented in offshore fields [8, 12, 36, 37]. Core and thin-sections investigations indicate that meteoric dissolution, dolomitization, cementation (calcite cementation and dominantly anhydrite cement), compaction, and fracturing are the most prominent and effective diagenetic processes [5, 16, 12, 37]. The extent and propagate of lithology, sedimentary environment, cement, and porosity of Kangan and Dalan formations in different rock units of the studied well are presented in a sedimentological and petrophysical log in Figure 7. Moreover, their comparative cross plots

are shown in Figure 8. The Figures show that each unit represents special characterization.

### The K1 Unit

The K1 unit with an apparent thickness of 100 m and average porosity of 6.6% is dominated by dolomite, with intercalations of anhydrite and mud to grain dominated limestones (Figure 7). Oomoldic porosity is the main pore type in limestone parts, while interparticle and intercrystalline porosities are attached to moldic pores in dolomitic parts and increased the reservoir quality. However, the formation of equant and coarse sparry calcite cement in limy parts and dolomite cement in dolomitic parts has reduced porosity and permeability of those related intervals (Figure 7); anhydrite cement is more frequent than carbonate cement, and it has extensively annihilated the reservoir quality.

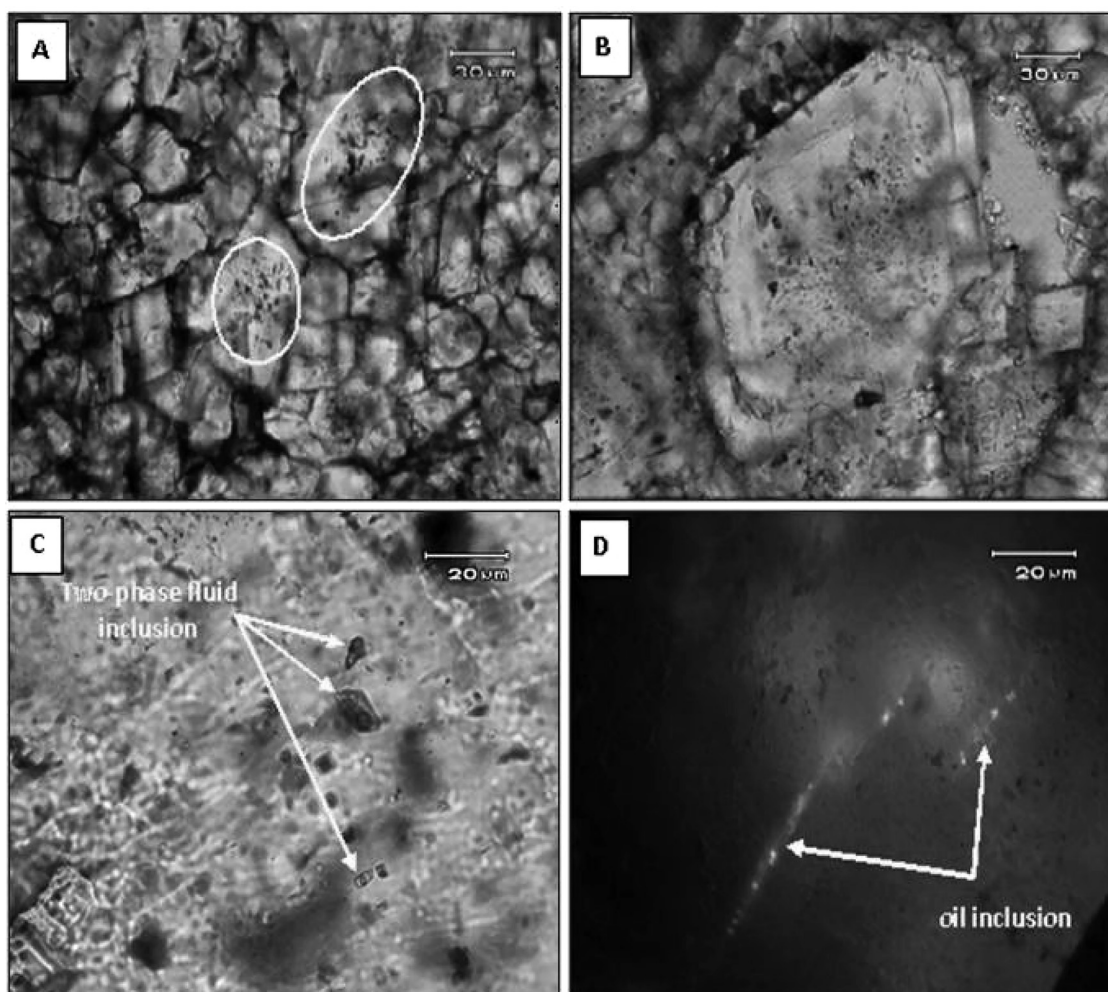


Figure 6: Photomicrographs of fluid and hydrocarbon inclusions within coarse crystalline cements in Kangan and Dalan Formations: A) indicates size in  $\mu\text{m}$  inclusions in pore-filling calcite cement, ppl. B) Small fluid inclusions in pore-filling dolomite cement, ppl. C) Medium to large two-phase fluid inclusions in fracture-filling calcite cement, ppl. D) Secondary hydrocarbon inclusions which formed along of micro cracks, UV light.

### The K2 Unit

The K2 unit with a thickness of 45 m commonly consists of thrombolite boundstones at the base, overlaid by thick shoal setting ooid grainstones, and thin intercalations of lagoon-peritidal mud dominated facies. The reservoir quality of this rock unit is enhanced toward the upper part of K2 significantly in ooidal grainstones (with average porosity of 9.3%). The abundance of equant and coarse sparry cements in the lower part of K2 has occluded the pore spaces, and has reduced the reservoir properties (Figure 7).

### The K3 Unit

The K3 unit is separated by thick anhydrite from the underlying K4. Rahimpour-Bonab [22] identified this anhydritic zone as a barrier to vertical fluid flow in this field. The prominent lithology is dolomite. Limestone is present in the lower and upper parts of K3. This unit mainly consists of lagoonal, shoal, slightly peritidal, and open marine facies (Figure 7). The frequency of calcitic and dolomitic cements is decreased, while the amount of anhydrite cement is increased and has notably reduced the reservoir quality (Figure 7).

## The K4 Unit

The K4 unit with a thickness of 135 m and average porosity of 5.5% is characterized by dolomitic intervals with anhydrite bed in the upper part (Figure 7). Dolo ooid grainstones in shoal setting with good reservoir qualities occur in the middle part of the unit. Intercrystalline, interparticle, and moldic porosities are common pore types. The K4 consists entirely of stacked and oomoldic grainstone/packstones [4, 11, 12]. Except for pore occluding anhydrite, carbonate cement is observed scarcely in this unit.

Comparative cross plots (Figures 8A-8D) represent the frequency and average of lithology, cement type, sedimentary environment, and porosity in defined rock units of Kangan and Dalan formations. The K2 unit is not as much as other units under dolomitization and has remained more as a limy part (Figures 7 and 8A). Calcite cements like isopachous, granular equant, and coarse blocky are developed commonly in calcareous part (unit K2), while dolomite cement and associated cement, i.e. anhydrite, has extended in the dolomitized units of K1, K3, and K4 (Figures 7 and 8B). The dominant lithology of the rock can have an effect on the binding agent in that rock. The rock-fluid interaction causes the ions transport and the precipitation of calcite or dolomite cement in the calcitic or dolomitic prevailing lithology respectively; however, the depositional facies and environment are also affected by cementation. As can be seen in Figure 8C, lagoonal facies have higher frequency in units K1, K3, and K4, and, due to their nature of muddy facies with high Mg calcite (HMC), they have been replaced by dolomite.

Oomoldic porosity has frequently been developed in ooidal grainstone as a result of meteoric diagenesis and dissolution (Figure 3B). Also, dolomitization

(intercrystalline porosity) may cause pore spaces (moldic and intercrystalline), and consequently porosity and permeability are focused on these intervals (units K1, K2, and K4) as shown in Figure 8D. The plot shows that the average porosity values in K2, K1, K4, and K3 decrease respectively. Meteoric dissolution (largely in ooid grainstones) is the most important diagenetic process in the generation of secondary porosity in the studied interval.

The history of different cementing phases and related dissolution in the Dalan and Kangan carbonates, following deposition, is shown in Figure 9.

## Interpretation

The interpretation of the petrographic and cathodoluminescence data in conjunction with data from fluid inclusion studies indicates a complex diagenetic history for the Kangan-Dalan deposits. It has been assumed that cathodoluminescence in carbonate rocks is mainly derived from the incorporation of manganese into the calcite lattice, with the ion commonly acting as a cathodoluminescence quencher [38]. The isopachous cement (C1) on skeletal and non-skeletal particles is generally interpreted as a typical of a marine phreatic environment, where all the pore spaces are filled with marine water [39]. The isopachous cement and their non-luminescent features, together with the fact that they occur as the first stage cement before compaction, would indicate a marine phreatic origin [40-41]. It is important to point out that luminescence is not only controlled by the variations in the  $Mn^{++}$  and the  $Fe^{++}$  fluid concentrations, but also by crystals growth rates [42]. The bright orange and yellow luminescence of equant C5 and C6 cements suggest that both should have had the same initial probably high magnesium calcite composition.

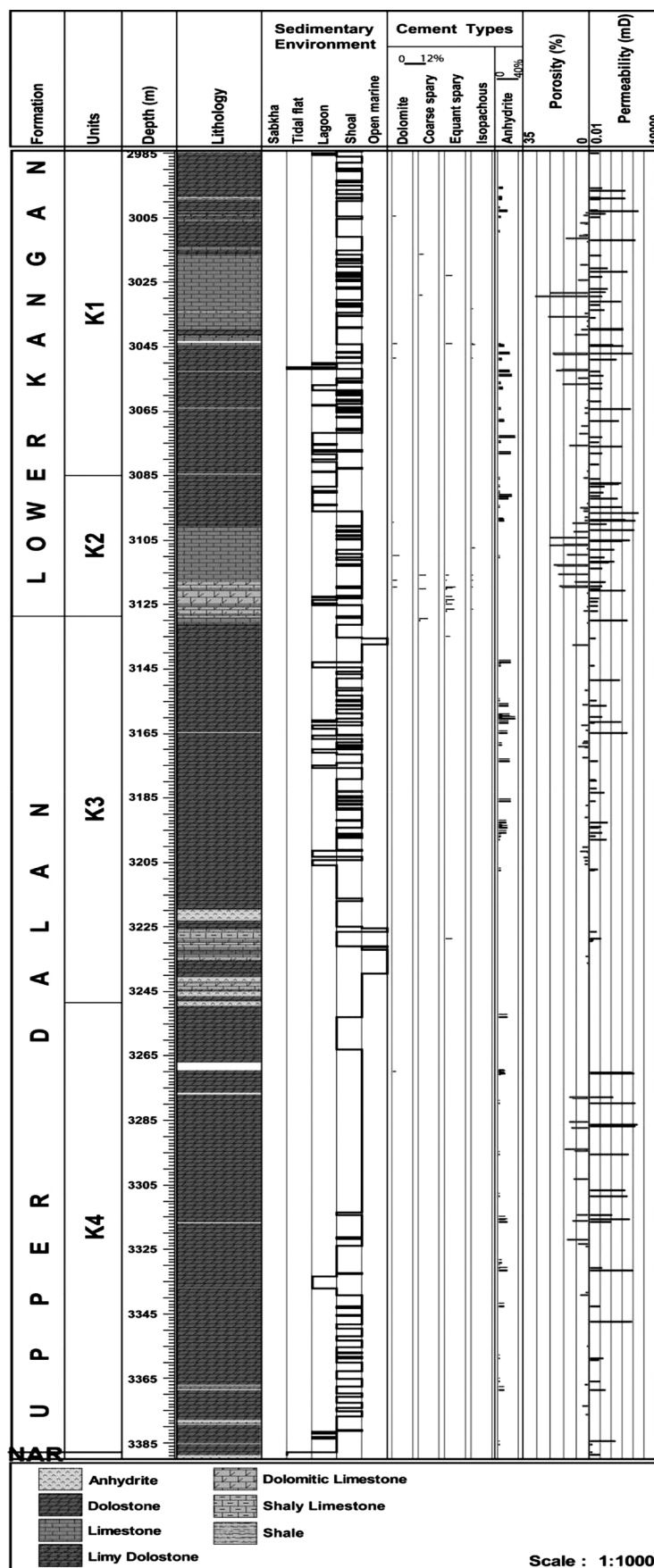


Figure 7: A Sedimentological and petrophysical log of Kangan and Dalan Formations.

Alternatively, the luminescence might be interpreted as having formed in the same way and at the same time on the basis of their similarity in the luminescence pattern; this might be produced by diagenetic alteration, as well as the luminescent features of the microspar calcite cement. The granular calcite cement has variable luminescent according to distinct color, which represents phases of crystal growth. In fact, each color represents the precipitation of calcite from pore waters with different chemical composition [43-44] from dull red (C2) luminescent (DL), to bright orange (C5) luminescent area (BOL), and to brightly yellow (C6) luminescent (BYL) zone. These variations in the luminescence characteristics are probably caused by the periodic incorporation of  $Mn^{++}$ . Irregular boundaries between alternating zones suggest rapid changes during the temporal interruption of crystal growth. Moreover, coarse blocky calcite (C4) in fractures and vugs with dull to non-luminescent together with distinct cleavage in large crystals could originate from the deep burial environment as the fluid inclusion reveals that this cement has precipitated from saline brines over a range of temperatures. It means that the fluids with higher temperature have migrated from deeper parts of the basin and have filled fractures during deep burial. It seems that hydrocarbon yellow inclusions are secondary; furthermore, they are distributed along micro cracks that can show the migration path, and it can be interpreted that hydrocarbon migration predates the precipitation of cements.

The dull/bright/yellow CL transition is generally interpreted as being caused by an increase in redox potential (Eh) under conditions of progressive marine burial meteoric-phreatic diagenetic environment [41]. This zonation in luminescence suggests geochemical variations within pore fluids system. The dull red CL cement (C2), under an anoxic condition and based

on the first group of fluid inclusion data, is a fluid with calcite composition and is interpreted to have precipitated during burial from pore water. However, the bright orange and yellow luminescence of granular calcite cements (C5 and C6) were probably precipitated under suboxic conditions [41], and it is understood that this type of cements occurred as a consequence of the influence of meteoric water. Leaching and neomorphism (microspar) occurred when meteoric waters were flowed through Kangan Dalan sediments during shallow burial. Cathodoluminescence reveals fine scale oscillatory zonation within granular calcite cement, which is more common in the Kangan Dalan succession. Dolomite cements, under both optical and cathodoluminescence microscopes, demonstrate zoning patterns, which, through the data achieved from vacuoles fluid with dolomite composition, was precipitated possibly during shallow burial to burial. Finally, the sediments originated as shallow marine mainly in a phreatic realm during the first stage of diagenesis. The second stage of diagenesis is interpreted to have occurred in a burial environment by the formation of equant (C2), dolomite (C3), and coarse sparry calcite (C4). The next phase of diagenesis is expected to have happened during meteoric-phreatic area by the precipitation of C5 and C6. The entry of waters will first dissolve aragonitic grains (bioclasts and ooids), and later the saturated waters induce the adjacent precipitation of a stable mineral phase as mosaic intergranular calcite (meteoric equant cement). However, the comparison of Figures 8B and 8D shows that increasing cements are associated to occluding depositional-dissolution related porosities of pertinent unit. In general, as Kangan and Dalan carbonates are buried more deeply, they are commonly in equilibrium with the adjacent subsurface waters; nevertheless, significant diagenetic changes can occur. Since different phases

of cementation (Figure 9) with various amounts have occurred, the associated phases of pore space filling in each rock unit have taken place. Therefore, the

creation and preservation of porosity as a function of fluid saturation in different units (Figure 8D) of the formation generally will be arisen.

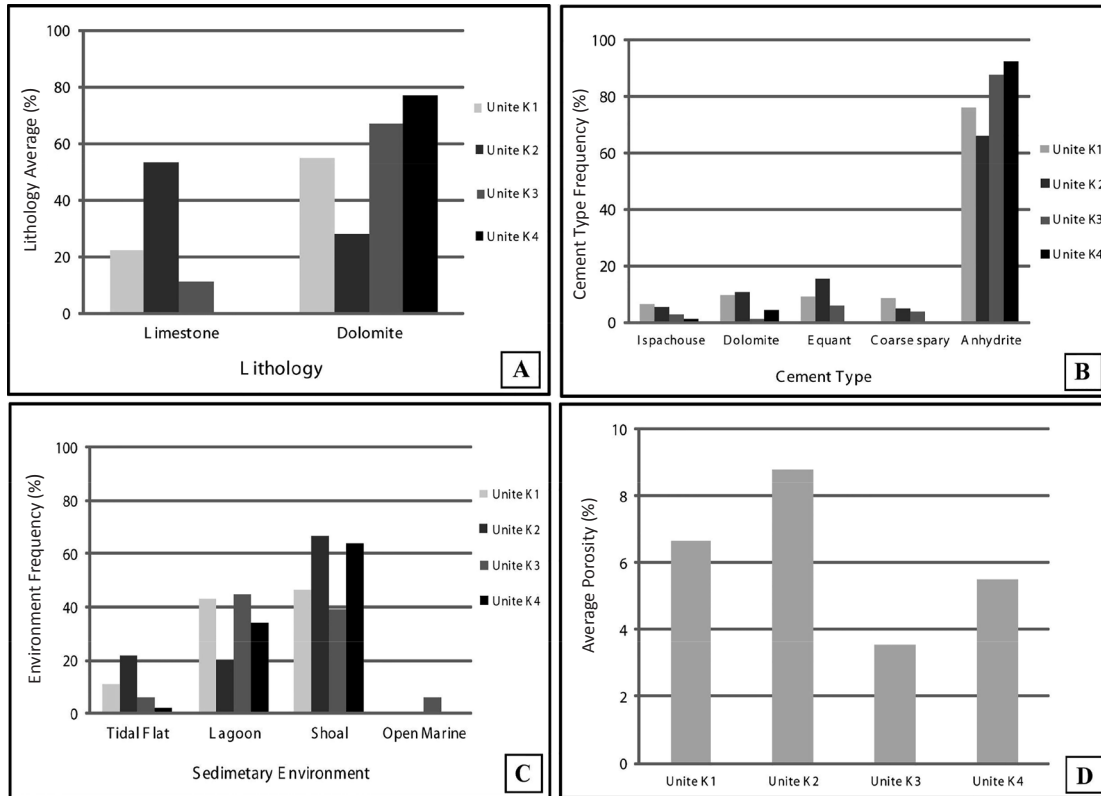


Figure 8: Cross plots of lithology, cement, sedimentary environment and porosity in different units of Kangan and Dalan Formations.

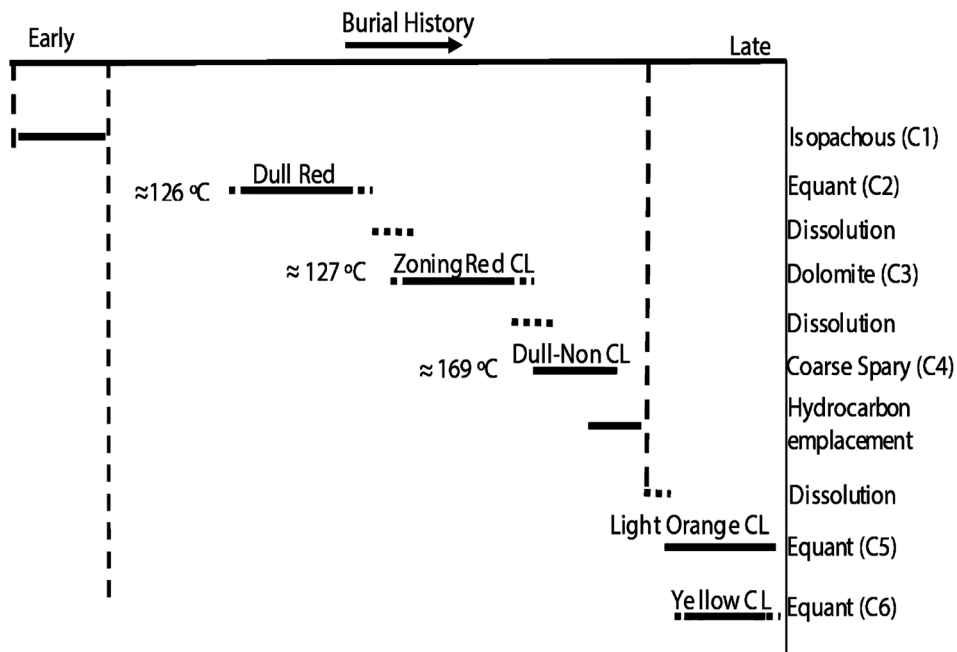


Figure 9: Diagenetic paragenesis of carbonate cement in Kangan and Dalan Formation.

## CONCLUSIONS

The Upper Permian–Triassic carbonate platform succession has undergone a complex diagenetic evolution, where several diagenetic phases have recorded in the initial depositional, shallow-deep, and uplift conditions.

Petrography and cathodoluminescence observations revealed that cement types appear to be (i) early granular isopachous calcite (C1) with nonluminescent CL precipitated as early alterations on the sea floor which could be syn-depositional and are interpreted as early marine cements.

The next diagenetic phases of the Kangan-Dalan formations can be summarized as (ii) burial equant calcite (C2-dull red CL), (iii) coarse secondary dolomite (100 < size micron) rhombs (C3-red zoning CL), (iv) burial coarse sparry calcite (C4-dull to non-luminescence). Finally, uplift can be identified by two types of meteoric cements including (v) equant with C5-bright orange CL and (vi) equant with C6-yellow CL. All these processes are indicative of changes from marine phreatic-freshwater to burial to uplift diagenetic conditions.

Fluid inclusion micro thermometric data on calcite and dolomite cements show an alternative trend of increasing and decreasing temperature and salinity through depth and time from shallow to late-burial diagenetic conditions. The high Th value of coarse sparry calcite (155.4 °C to 181.2 °C) is interpreted as fluid migration from deeper parts of the basin and filling fractures during deep burial. Dolomitizing fluid was precipitated possibly during shallow burial and through calcitizing fluids, and equant cements (C5, C6) have precipitated from pore fluids influenced by meteoric water.

Hydrocarbon inclusions were observed only in Dalan formation, and it seems that they are secondary; hydrocarbon migration predates the precipitation of

coarse calcite cements. Thus, this study shows that there is some post migration diagenesis which is caused by an unsteady state hydrocarbon migration. Reservoir properties result from the original sedimentary texture and diagenesis. Average porosity values differ from 3.5% in the K3 to 10% in the K2 units, made up of fine to coarse ooidal packstone to grainstone. The early to late diagenetic dissolution of the ooids and cement can presumably account for a significant amount of porosity formation of the studied Permian-Triassic Dalan-Kangan reservoirs.

## ACKNOWLEDGMENTS

The authors would like to thank the Research Institute of Petroleum Industry (RIPI) for providing us with cathodoluminescence and fluid inclusion laboratory equipment for the examination. We extend our appreciation to the Petropars Oil Company for permission to publish the result of this paper. This research was financially supported by RIPI. The authors are also grateful to Mr. Motiei, Dr. Nader (Institute de France du Petrol), and Mr. Kasaei for improving the manuscript with their critical reviews and suggestions.

## REFERENCES

1. Aleali M., Rahimpour-Bonab H., Moussavi-Harami R., and Jahani D., "Environmental and Sequence Stratigraphic Implications of Anhydrite Textures: A Case from the Lower Triassic of the Central Persian Gulf," *Journal of Asian Earth Sciences*, **2013**, 75, 110-125.
2. Ghazban F., "Petroleum Geology of the Persian Gulf," *Tehran University and National Iranian oil Company Publications*, **2007**, 707.
3. Kashfi M. S., "Greater Persian Gulf Permian-Triassic Stratigraphic Nomenclature Requires Study," *Oil and Gas Journal*, **2000**, 6, 36-44.
4. Esrafil-Dizaji B. and Rahimpour-Bonab H., "A

- Review of Permian-Triassic Reservoir Rocks in the Zagros Rrea, Southwest of Iran: Influence of the Qatar-Fars arch," *Journal of Petroleum Geology*, **2013**, 36(3), 257-279.
5. Moradpour M., Zamani Z. and Moallemi S. A., "Controls on Reservoir Quality in the Lower Triassic Kangan Formation, Southern Persian Gulf," *Journal of Petroleum Geology*, **2008**, 31(4), 367-385.
  6. Fontana S., Nader, F.H., Morad S., Ceriani A., et al., "Fluid-rock Interactions Associated with Regional Tectonics and Basin Evolution," *Sedimentology*, **2014**, 61(3), 660-690.
  7. Fontana S., Nader F. H., Morad S., Ceriani A., et al., "Diagenesis of the Khuff Formation (Permian-Triassic), Northern United Arab Emirates," *Arab J. Geosci.*, **2010**, 3, 351-368.
  8. Ehrenberg S. N., "Porosity Destruction in Carbonate Platforms," *Journal of Petroleum Geology*, **2006**, 29, 41-52.
  9. Neilson J. E. and Oxtoby N. H., "The Relationship between Petroleum, Exotic Cements and Reservoir Quality in Carbonates, A review," *Marine and Petroleum Geology*, **2008**, 25, 778-790.
  10. Rahimpour-Bonab, H., "A Procedure for Appraisal of a Hydrocarbon Reservoir Continuity and Quantification of its Heterogeneity," *Journal of Petroleum Science and Engineering*, **2007**, 58, 1-12.
  11. Esrafil-Dizaji B. and Rahimpour-Bonab H., "Effects of Depositional and Dagenetic Characteristics on Carbonate Reservoir Quality: a Case Study from the South Pars Gas Field in the Persian Gulf," *Petroleum Geoscience*, **2009**, 15, 325-344.
  12. Rahimpour-Bonab H., Esrafil-Dizaji B., and Tavakoli V., "Dolomitization and Anhydrite Precipitation in the Permian-Triassic Carbonates at the South Pars Gas Field, Offshore Iran: Controls on Reservoir Quality," *Journal of Petroleum Geology*, **2010**, 33, 43-66.
  13. Ameen M. S., Buhidma I. M., and Rahim Z., "The Function of Factures and in-situ Stresses in the Khuff Reservoir Performance, Onshore Fields, Saudi Arabia," *AAPG Bulletin*, **2010**, 94, 27-60.
  14. Koehrer B., Zeller M., Aigner T., Poeppelreiter M., et al., "Facies and Stratigraphic Framework of a Khuff Outcrop Equivalent: Saiq and Mahil Formations, Al Jabal al-Akhdar, Sultanate of Oman," *GeoArabia*, **2010**, 15, 91-156.
  15. Koehrer B., Aigner T. and Pöppelreiter M., "Field-scale Geometries of Upper Khuff Reservoir Geobodies in an Outcrop Analogue (Oman Mountains, Sultanate of Oman)," *Petroleum Geoscience*, **2011**, 17, 3-16.
  16. Insalaco E., Virgone A., Courme B., Gaillot J., et al., "Upper Dalan member and Kangan Formation between the Zagros Mountains and offshore Fars, Iran: Depositional System, Biostratigraphy and Stratigraphic Architecture," *GeoArabia*, **2006**, 11(2), 75-176.
  17. Edgell H. S., "Salt Tectonism in the Persian Gulf Basin, In: Asop, (Eds.)," *Salt Tectonics, Geological Society of London, Special Publication*, **1996**, 100, 51-129.
  18. Szabo F. and Kheradpir A., "Permian and Triassic stratigraphy of the Zagros Basin, Southwest Iran," *Journal of Petroleum Geology*, **1978**, 1, 57-82.
  19. Dickson J. A. D., "Carbonate Identification and Genesis as Revealed by Staining," *Journal of Sedimentary Petrology*, **1966**, 36(2), 491-505.
  20. Burruss R. C., "Practical Aspects of Fluorescence Microscopy of Petroleum Fluid Inclusions," *Luminescence Microscopy and Spectroscopy, Society of Economic Paleontologists and Mineralogists Short Course*, **1991**, 25, 1-7.
  21. Goldstein R. H., "Fluid Inclusions in Sedimentary

- and Diagenetic Systems," *Lithos*, **2001**, *55*, 159-193.
22. Goldstein R. H. and Reynolds T. J., "Systematics of Fluid Inclusions in Diagenetic Minerals: Society of Economic Paleontologists and Mineralogists," *Short Course*, **1994**, *31*, 199 .
  23. Bodnar R. J., "Revised Equation and Table for Freezing Point Depressions of H<sub>2</sub>O-salt Fluid Inclusions (Abstract): PACROFI," *4<sup>th</sup> Biennial Pan-American Conference on Research on Fluid Inclusions*, Program and Abstracts, Lake Arrowhead, **1992**, *14*, 15.
  24. Ali S. A., Clark W. J., and Moore W. R., "Diagenesis and Reservoir Quality, Oilfield Review," *Schlumberger*, **2010**, *22*(2).
  25. Bjorlkkey K., "Petroleum Geoscience: from Sedimentary Environments to Rock Physics," *Springer*, **2010**, 508.
  26. Mackenzie F. T., "Sediments, Diagenesis, and Sedimentary Rocks," *Elsevier*, **2005**, 448.
  27. Moore C. H., "Carbonate Diagenesis and Porosity," *Elsevier*, **1989**, 338.
  28. Palma R. M., Bressan G. S., and Kietzmann D. A., "Diagenesis of a Bioclastic Oyster Deposit from the Lower Cretaceous (Chachao Formation), Neuquen Basin, Mendoza Province, Argentina," *Carbonates and Evaporites*, **2008**, *23*(1), 39-49.
  29. Tucker M. E. and Wright V. P., "Carbonate Sedimentology," Blackwell Scientific Publications, Oxford, **1990**, 497.
  30. Flugel E., "Microfacies of Carbonate Rocks, Analysis, Interpretation and Application," 2<sup>nd</sup> edition, *Springer*, **2010**, 984.
  31. Longman M. W., "Carbonate Diagenetic Textures from Near Surface Diagenetic Environments," *AAPG Bulletin*, **1980**, *64*, 461-487.
  32. Scoffin T. P., "Introduction to Carbonate Sediments and Rocks," Chapman and Hall, New York, **1987**, 274.
  33. McLimans R. K., "The Application of Fluid Inclusions to Migration of Oil and Diagenesis in Petroleum Reservoirs," *Applied Geochemistry*, **1987**, *2*(5-6), 585-603.
  34. Dasgupta S. N., Hong M., and Al-Jallal I. A., "Accurate Reservoir Characterization to Reduce Drilling Risk in Khuff-C Carbonate, Ghawar field, Saudi Arabia," *GeoArabia*, **2002**, *7*, 81-100.
  35. Alsharhan A. S., "Sedimentological Character and Hydrocarbon Parameters of the Middle Permian to Early Triassic Khuff Formation, United Arab Emirates," *Geo Arabia*, **2006**, *11*, 121-158.
  36. Tavakoli V., Rahimpour-Bonab H. and Esrafil-Dizaji B., "Diagenetic Controlled Reservoir Quality of South Pars Gas Field, an Integrated Approach," *Comptes Rendus Geoscience*, **2010**, *343*, 55-71.
  37. Peyravi M., Kamali M. R., and Kalani M., "Depositional Environments and Sequence Stratigraphy of the Early Triassic Kangan Formation in the Northern Part of the Persian Gulf: Implications for Reservoir Characteristics," *Journal of Petroleum Geology*, **2010**, *33*, 371-386.
  38. Meyers W. J., "Carbonate Cement Stratigraphy of the Lake Valley Formation (Mississippian) Sacramento Mountains, New Mexico," *Journal of Sedimentary Petrology*, **1974**, *44*, 837-861.
  39. Prezbindowski D. R., "Burial Cementation, Is It Important? A Case Study, Stuart City Trend, South Central Texas," *Society of Economic Paleontologists and Mineralogists*, Special Publication, **1985**, *36*, 241-264.
  40. Frank J. R., Carpenter A. B., and Oglesby W., "Cathodoluminescence and Composition of Calcite Cement in the Taum Sauk Limestone (Upper Cambrian), Southeast Missouri," *Journal of Sedimentary Petrology*, **1982**, *52*, 631-638.
  41. Grover G. and Read J. F., "Paleoaquifer and Deep Burial Related Cements Defined by

Regional Cathodoluminescence Patterns, Middle Ordovician Carbonates, Virginia," *AAPG Bulletin*, **1983**, *67*, 1275-1303.

42. Reeder R. J. and Grams J. C., "Sector Zoning in Calcite Cement Crystals: Implications for Trace Elements Distributions in Carbonates," *Geochimica et Cosmochimica Acta*, **1987**, *51*, 187-194.
43. Meyers W. J., "Calcite Cement Stratigraphy: an Overview," *SEPM Short Course*, **1991**, *25*, 133-148.
44. Machel H. G., "Application of Cathodoluminescence to Carbonate Diagenesis" Springer-Verlag, Heidelberg, **2000**, 271-301.